Surface effects on the mechanical properties of nanoporous materials

2011 Nanotechnology 22 265714

(http://iopscience.iop.org/0957-4484/22/26/265714)

Nanotechnology **22** (2011) 265714 (7pp) doi:10.1088/0957-4484/22/26/265714

Surface effects on the mechanical properties of nanoporous materials

Re Xia[1,2], Xide Li[2], Qinghua Qin[3], Jianlin Liu[4] and Xi-Qiao Feng[2]

[1] School of Power and Mechanical Engineering, Wuhan University, Wuhan 430072, People's Republic of China
[2] AML, Department of Engineering Mechanics, Tsinghua University, Beijing 100084, People's Republic of China
[3] School of Engineering, Australian National University, Canberra, ACT 0200, Australia
[4] Department of Engineering Mechanics, China University of Petroleum, Qingdao 266555, People's Republic of China

E-mail: fengxq@tsinghua.edu.cn

Received 1 February 2011
Published 18 May 2011
Online at stacks.iop.org/Nano/22/265714

Abstract
Using the theory of surface elasticity, we investigate the mechanical properties of nanoporous materials. The classical theory of porous materials is modified to account for surface effects, which become increasingly important as the characteristic sizes of microstructures shrink to nanometers. First, a refined Timoshenko beam model is presented to predict the effective elastic modulus of nanoporous materials. Then the surface effects on the elastic microstructural buckling behavior of nanoporous materials are examined. In particular, nanoporous gold is taken as an example to illustrate the application of the proposed model. The results reveal that both the elastic modulus and the critical buckling behavior of nanoporous materials exhibit a distinct dependence on the characteristic sizes of microstructures, e.g. the average ligament width.

(Some figures in this article are in colour only in the electronic version)

1. Introduction

Nanoporous materials have many attractive physical and mechanical properties, e.g. high yield strength, good electrocatalytic performance, strong surface-enhanced Raman scattering, charge-induced reversible strain, surface-chemistry-driven deformation and very small electrical resistance in external magnetic fields [1–7], and therefore hold great promise for a diversity of technologically important applications. In addition, the mechanical behavior of some nanoporous materials shows an evident dependence on the characteristic sizes of the microstructure [8–10]. All these features of nanoporous materials are, more or less, attributed to their nanosized structure consisting of either open or closed pores. In the classical theory for porous materials, however, the mechanical properties are assumed to be independent of the structure scale. In other words, porous solids with the same statistically averaged characteristic parameters (e.g. relative density, pore distribution and bulk material modulus) would exhibit identical mechanical properties, no matter whether their average ligament size is at the macro-, meso-, micro- or nanoscale [11, 12]. Therefore, although the classical theory of porous materials has been widely used to design their microstructures and to predict the corresponding mechanical properties, it becomes inaccurate or invalid in dealing with the same problems for nanoporous materials.

Recently, much effort has been directed towards understanding the size-dependent elasticity of porous materials with very small ligament or pore size. In particular, the surface effects on their unusual mechanical behavior have been examined [13–15]. These previous studies provided a reasonable explanation for some relevant experimental results. However, the existing theoretical models based on the Euler–Bernoulli beam model are valid mainly for porous materials with a very low relative density [1–10]. When the average aspect ratio between the length to width of ligaments is relatively small, the effects of transverse shear force and rotary inertia will have a pronounced influence on the deformation of microstructures and should be taken into account [16]. In this case, the Timoshenko beam model can be used to analyze the

mechanical behavior of ligaments in nanoporous materials with a comparatively high mass density [17]. Recently, therefore, the Timoshenko beam theory and its various modified forms have been employed to predict the size-dependent mechanical properties of nanobeams and nanotubes [18–20]. To date, nevertheless, there is still a lack of theoretical investigation on the properties of nanoporous materials.

In this paper, we investigate the influences of surface effects on the mechanical properties of nanoporous materials by using the theory of surface elasticity. The modified Timoshenko beam theory is first formulated by incorporating surface effects and then used to predict the effective elastic modulus of high-density nanoporous materials. The elastic buckling of nanoporous materials with surface effects is also analyzed.

2. Theory of surface elasticity

In the past few decades, several theories have been developed to theoretically explore the size effects of small-scale materials. For example, the strain gradient theory, proposed by Mindlin and Eshel [21] and expanded by Fleck and Hutchinson, can reasonably explain some size-dependent experimental phenomena with large plastic strain gradients [22]. The microcontinuum theory elaborated by Eringen [23] has a simpler type with a micropolar continuum. It treats the microrotations as independent degrees of freedom in addition to the usual linear displacements. Using this scale-based model, size effects in the bending deformation of nanowires and carbon nanotubes have been elucidated [24]. The nonlocal elasticity theory initiated by Eringen and Edelen [25] has also been adopted to predict the size-dependent phenomena of small-scale structures, by assuming that the stresses at a point depend not only on the strain at that point but also on the strain field in the whole body. This theory has been successfully applied to study wave propagation, dislocations, crack propagations, vibration, buckling and other micro/nanoscale devices [20, 26, 27]. The theory of surface elasticity, proposed by Gurtin *et al* [28], is another efficient continuum theory for analyzing size-dependent problems, especially those observed at the nanoscale. Recently, this continuum theory has been employed to interpret many size-dependent phenomena of nanoscale materials, observed in experiments and atomistic simulations [29–34]. For completeness, the theory of surface elasticity will be briefly reviewed in this section and it will be used to investigate the mechanical behavior of nanoporous materials.

Since near-surface atoms of a material reside in a local environment different from that in the interior, the surface layer, typically with a thickness of ∼1 nm, has mechanical properties and an energy density different from its bulk counterpart [35]. In the theory of surface elasticity [28], a surface is normally viewed as a two-dimensionally heterogeneous thin film attached to its bulk. The fundamental equations in the bulk are identical to those in the classical theory of elasticity, except that the boundary conditions need to be modified to account for the effects of surface stresses. The surface layer and the bulk material are assumed to be bonded perfectly so that their displacements are continuous across the interface. Thus, the equilibrium equation and its non-classical boundary conditions can be written as [29, 33]

$$\tau_{\alpha\beta,\beta} + t_\alpha = 0, \qquad \tau_{\alpha\beta} k_{\alpha\beta} = \sigma_{ij} n_i n_j, \tag{1}$$

respectively, where n_i is the unit normal vector of the surface layer, t_α the tangential component of the traction $\sigma_{ij} n_j$ along the α direction, $k_{\alpha\beta}$ the curvature tensor of the surface and $\tau_{\alpha\beta}$ the surface stress tensor. Throughout this paper, Einstein's summation convention is adopted for all repeated Latin indices (1, 2, 3) and Greek indices (1, 2).

It can be seen from equation (1) that the volume stress has a jump at the surface but the condition of displacement continuity holds true. In an Eulerian framework, the surface stress tensor $\tau_{\alpha\beta}$ and the surface energy density λ satisfy the Shuttleworth equation:

$$\tau_{\alpha\beta} = \lambda \delta_{\alpha\beta} + \frac{\partial \lambda}{\partial \varepsilon_{\alpha\beta}}, \tag{2}$$

where $\varepsilon_{\alpha\beta}$ is the in-plane component of the bulk strain tensor at the surface. Equation (2) provides a two-dimensional constitutive relation of a surface. For simplicity, suppose that both the surface layer and the bulk material are isotropic and linearly elastic, and that the surface layer has the uniform thickness t_0 and Young's modulus E_t. Hence the constitutive relation of a surface can be written as

$$\tau_{\alpha\beta} = \tau^0_{\alpha\beta} + S_{\alpha\beta\gamma\delta} \varepsilon_{\gamma\delta}, \tag{3}$$

where $\varepsilon_{\gamma\delta}$ is the surface strain tensor, $S_{\alpha\beta\gamma\delta}$ is the surface elastic constant tensor and $\tau^0_{\alpha\beta}$ is the residual surface stress tensor when the bulk strain is zero. For a one-dimensional problem, equation (3) reduces to [29, 34]

$$\tau = \tau_0 + E_s \varepsilon_x, \tag{4}$$

where τ is the surface stress, ε_x is the surface stress in the x direction, $E_s = E_t t_0$ is the effective surface Young's modulus and τ_0 is the residual surface stress.

3. Timoshenko's beam model with surface effects

According to the well-known Gibson–Ashby foam theory [11, 12], an open-cell nanoporous foam can be considered as a three-dimensional structure consisting of a large number of identical unit cells periodically arranged along three dimensions. Further, the unit cell can be viewed as a nanoscale structure composed of a certain number of nanobeams. To explore the elastic properties of such a nanoporous material, a theoretical approach is developed based on the bottom-up methodology in this paper. First, we present a refined Timoshenko's beam model to account for both the effects of surfaces and shear deformation. This model allows us to analyze the deformation of the ligaments in the unit cells of a nanoporous material.

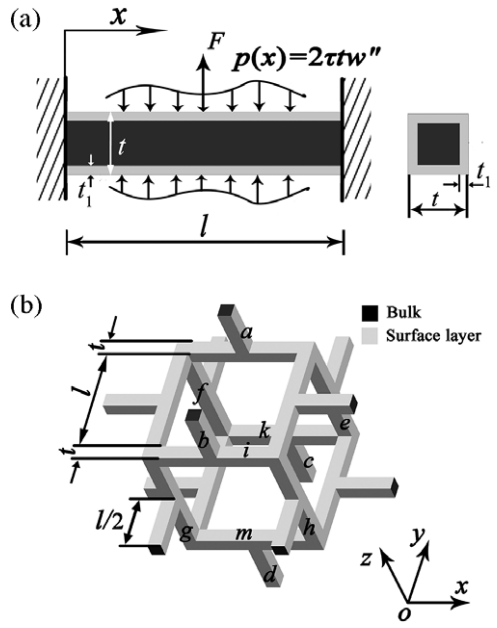

Figure 1. (a) Timoshenko nanobeam model accounting for surface effects. (b) Unit-cell model for open-cell nanoporous materials.

3.1. Surface effects on the bending of a Timoshenko nanobeam

Recently, the size-dependent elastic behavior of nanowires has been successfully interpreted by accounting for the effects of surface stresses and surface elasticity. In these previous studies, the classical Euler–Bernoulli beam model was often used, which assumes a large length l to width t ratio and only considers the influence of bending deformation. When the nanobeam has a relatively small aspect ratio of l/t, it is necessary to include both the pure bending and the additional effect caused by shear deformation [16]. Thus, we will adopt the Timoshenko nanobeam model in this study.

The governing equation for a bending Timoshenko beam is given as

$$w' = \theta + \gamma \tag{5}$$

where w is the deflection, θ the slope of the beam centerline and γ the shear angle. The shear force against the internal shear loading is

$$Q = -\kappa GA\gamma = -\kappa GA(w' - \theta) \tag{6}$$

where κ is the shear coefficient, G the shear modulus and A the cross-sectional area. For a beam with a square section, one has $A = t^2$ and $\kappa = 5(1+v)/(6+5v)$, where v is the Poisson ratio of the material [17].

Now we consider a doubly clamped Timoshenko nanobeam by accounting for the effects of surface stresses and surface elasticity, as shown in figure 1(a). In the case of small displacements, the residual surface tension can be treated as a distributed transverse loading $p(x)$ along the longitudinal direction of the nanobeam according to the Laplace–Young equation [30–32]:

$$p(x) = Hw'', \tag{7}$$

where H is a constant determined by the surface stress and the cross-sectional shape. H is approximately taken as $H_0 = 2\tau_0 t$ for a rectangular cross section [14, 30, 31]. Assume that the surface layer thickness t_0 is much smaller than the thickness t of the bulk layer. The effective bending moment of nanobeam $(EI)^*$ is [30, 31]

$$(EI)^* = \tfrac{1}{12}E_0t^4 + \tfrac{2}{3}E_st^3, \tag{8}$$

where E_0 is the Young's modulus of the bulk material.

When a doubly clamped nanobeam is subjected to a concentrated load F at its middle, the corresponding energy functional Π is written as

$$\prod = \int_0^{l/2} (EI)^*(\theta')^2\,\mathrm{d}x + \int_0^{l/2} V(w'-\theta)^2\,\mathrm{d}x - 2\int_0^{l/2} p(x)w\,\mathrm{d}x - Fw(l/2) \tag{9}$$

where $V = \alpha Gt^2$ is the shear stiffness. The variation of equation (9) gives

$$\begin{aligned}\delta\prod = {} & 2\int_0^{l/2} (EI)^*\theta'\delta\theta'\,\mathrm{d}x + 2\int_0^{l/2} V(w'-\theta)(\delta w'-\delta\theta)\,\mathrm{d}x \\ & - 2\int_0^{l/2} p(x)\delta w\,\mathrm{d}x - F\delta w(l/2) = 2[(EI)^*\theta'\delta\theta]_0^{l/2} \\ & - \int_0^{l/2} (EI)^*\theta''\delta\theta\mathrm{d}x + [V(w'-\theta)\delta w]_0^{l/2} \\ & - 2\int_0^{l/2} V(w''-\theta')\delta w\,\mathrm{d}x - 2\int_0^{l/2} V(w'-\theta)\delta\theta\,\mathrm{d}x \\ & - 2\int_0^{l/2} p(x)\delta w\,\mathrm{d}x - F\delta w(l/2).\end{aligned} \tag{10}$$

According to the principle of minimum potential energy, i.e. $\delta\prod = 0$, the Euler–Lagrange equations of the deformed nanobeam are obtained as

$$V(w''-\theta') + p(x) = 0, \qquad (EI)^*\theta'' + V(w'-\theta) = 0. \tag{11}$$

Due to the action of the concentrated force, the shear force $Q(x)$ has an abrupt change at the midpoint of the nanobeam. We get the force equilibrium condition

$$V[w'_{(l/2)} - w'_{(l/2)^+}] = F. \tag{12}$$

The symmetry of the nanobeam system leads to

$$Q^{\pm}(x) = V[w'_{(l/2)^{\pm}} - \theta_{(l/2)}], \qquad Q^-(x) = -Q^+(x). \tag{13}$$

Using equations (13), the force equilibrium condition in equation (2) for a Timoshenko nanobeam is simplified as

$$2V[w'_{(l/2)} - \theta_{(l/2)}] = F. \tag{14}$$

The natural boundary conditions are $w_{(0)} = \theta_{(0)} = \theta_{(l/2)} = 0$.

Solving equations (11) under the corresponding boundary conditions, the displacement function of a doubly clamped nanobeam with the coupling effects of surface stress ($H_0 \neq 0$) and shear deformation is derived as

$$w_{(x)} = \frac{F}{2H_0V\xi}\left[(H_0+V)\xi x - V\tanh(l\xi/4) + V\frac{\sinh(l\xi/4 - x\xi)}{\cosh(l\xi/4)}\right], \qquad (x \in [0, l/2]), \tag{15}$$

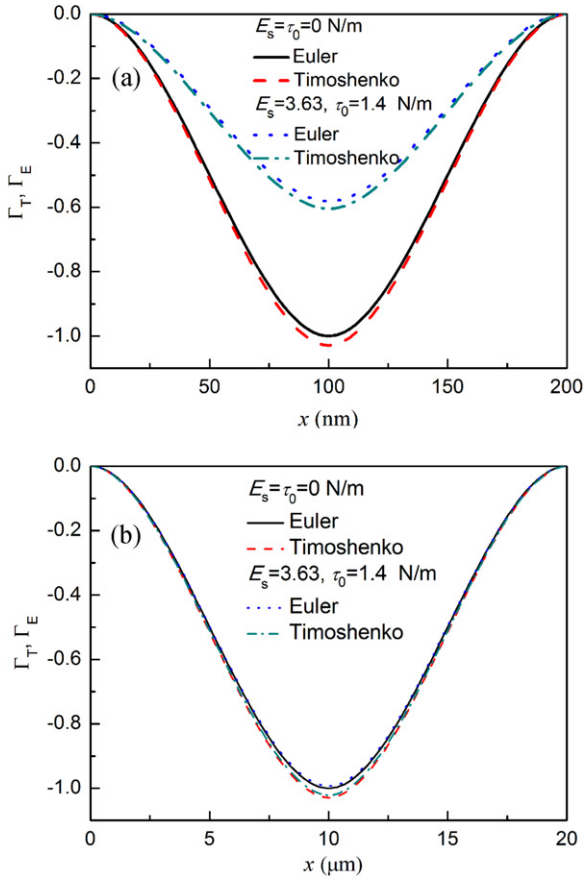

Figure 2. Comparison of the deflection curves predicted by Euler–Bernoulli model and Timoshenko model for a nanobeam with a high length–width ratio of 20 and the width (a) $t = 10$ nm and (b) $t = 1$ μm.

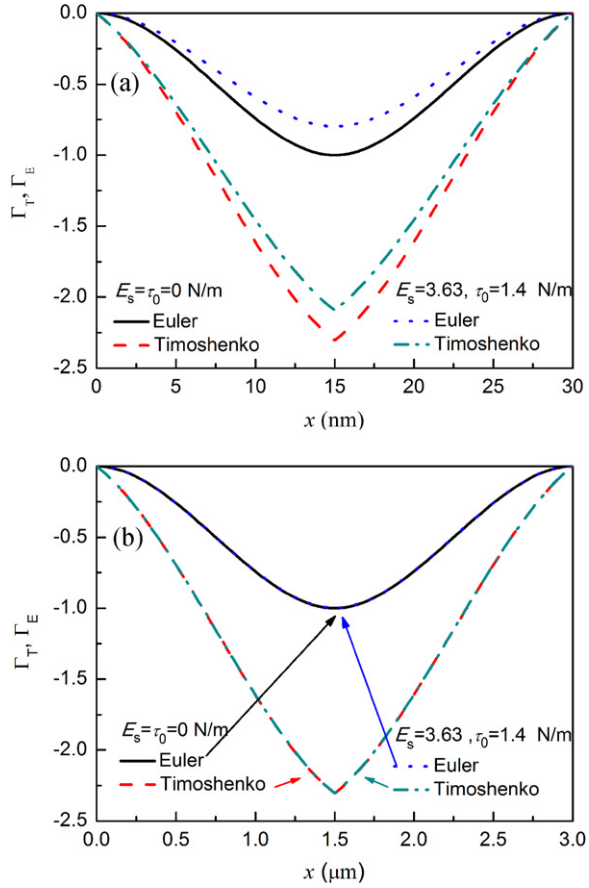

Figure 3. Comparison of the deflection curves predicted by Euler–Bernoulli model and Timoshenko model for a nanobeam with a high length–width ratio of 3 and the width (a) $t = 10$ nm and (b) $t = 1$ μm.

where $\xi = 1/\sqrt{(EI)^*(1/H_0 + 1/V)}$. If the surface stress effects are negligible (i.e. $H_0 = \tau_0 = 0$), the solution in equation (15) reduces to

$$w_{(x)} = Fx\left[\frac{(3l - 4x)x}{48(EI)^*} + \frac{1}{2V}\right], \qquad (x \in [0,\ l/2]). \tag{16}$$

In addition, ignoring the effect of shear deformation and letting the shear stiffness approach infinity (i.e. $V = \kappa GA \to \infty$), equations (15) and (16) will reduce to the solution for an Euler–Bernoulli nanobeam with surface effects derived in [31].

3.2. Comparison of surface effects on Timoshenko and Euler–Bernoulli nanobeams

To illustrate the difference between the Timoshenko and Euler–Bernoulli nanobeam models accounting for surface effects, a doubly clamped nanobeam subjected to a transversely concentrated force at the middle point is taken as an example. Nanoporous Au (NPG), as a well-known material in this category, is a particular candidate for studying the mechanical behavior of nanoporous metals due to its easy fabrication and remarkable stability against corrosion and oxidation [8, 9, 30]. The material parameters of single-crystalline bulk Au are taken as follows: bulk Young's modulus $E_0 = 70$ GPa, shear modulus $G = 27.2$ GPa, Poisson's ratio $v = 0.42$, surface Young's modulus $E_s = 3.63$ N m^{-1} and residual surface stress $\tau_0 = 1.4$ N m^{-1} in the (001) plane [36]. In use of equations (15) and (16), we introduce the following dimensionless deflections of the nanobeam predicted by the Euler–Bernoulli model and the Timoshenko model:

$$\Gamma_{\mathrm{E}} = w_{\mathrm{Euler}}/w_{(l/2)}, \qquad \Gamma_{\mathrm{T}} = w/w_{(l/2)}, \tag{17}$$

respectively, where w_{Euler} is the deflection of an Euler nanobeam with surface effects [30] and $w_{(l/2)} = Fl^3/(192EI)$ is the deflection at the midpoint. The deflection predicted by the two models are compared in figures 2 and 3, where we set the width of the nanobeam t =10 nm and the aspect ratio $l/t = 3$ and 20, respectively.

It can be found from figure 1 that the difference between the results predicted by the two models is negligible when the aspect ratio of the nanobeam, l/t, is larger than 3.0. Figure 3 shows that, for a smaller aspect ratio, the effect of shear deformation has a distinct influence on the deflection of the nanobeam. The displacement predicted by the Timoshenko nanobeam model is larger than that by the Euler–Bernoulli model.

In addition, figure 2 shows that the deflection of the nanobeam decreases with the increase in the surface stress,

indicating that a positive surface stress will make the nanobeam stiffer. Therefore, both the effects of surfaces and shear deformation distinctly affect the deformation behavior of nanobeams with a small aspect ratio. The smaller the characteristic sizes and the aspect ratio, the greater the influences of surface and shear deformation effects.

4. Effective elastic modulus of high-density nanoporous materials

4.1. Expression of effective elastic modulus

The elastic properties of nanoporous materials have been studied recently by adopting the Euler–Bernoulli beam model, which holds for materials with a very low mass density because of its neglect of shear deformation effects [13–15]. However, most practical nanoporous materials have a relatively higher density. For example, nanoporous gold fabricated by such techniques as alloy corrosion has a relative mass density ρ/ρ_0 in the range of 0.35–0.42 [1–10]. For such materials with a relatively higher density, the Timoshenko nanobeam model is more appropriate for the deformation analysis of ligaments than the Euler–Bernoulli beam model.

To predict the elastic modulus of nanoporous materials in terms of microstructural parameters, a unit-cell model containing a surface layer is introduced [14], as shown in figure 1(b). In this study, the four ligaments (i, j, k, m) in group (iii) are treated as Timoshenko nanobeams subjected to a force F at their midpoints. Thus the transverse displacement at the midpoint $w_{(l/2)}$ of a ligament can be obtained from equations (15) and (16) as

$$w_{(l/2)} = \begin{cases} Fl\left[\dfrac{l^2}{192(EI)^*} + \dfrac{1}{2V}\right], & \text{for } \tau_0 = 0, \\ \dfrac{F}{4H_0V\xi}\left[(H_0+V)\,l\xi - 4V\tanh\left(\dfrac{l\xi}{4}\right)\right], & \text{for } \tau_0 \neq 0. \end{cases} \tag{18}$$

Following the procedure in [14], the total averaged strain $\bar{\varepsilon}^*$ and the effective Young's modulus E^* of the high-density nanoporous material are respectively written as

$$\bar{\varepsilon}^* = \begin{cases} \dfrac{Fl^3}{192\,(EI)^*\,(l+t)} + \dfrac{F(2ltB+3lV+2tV)}{4VBt}, \\ \qquad \text{for } \tau_0 = 0, \\ \dfrac{F}{H_0(l+t)}\left[\dfrac{l(H_0+V)}{4V} - \dfrac{\tanh(l\xi/4)}{\xi}\right] \\ \qquad + \dfrac{F(3l+2t)}{4Bt(l+t)}, \qquad \text{for } \tau_0 \neq 0, \end{cases} \tag{19}$$

and

$$E^* = \begin{cases} \dfrac{96(EI)^*BV}{l^2tVB + 48(EI)^*(2ltB+3lV+2tv)}, & \text{for } \tau_0 = 0 \\ \dfrac{2BH_0V\xi}{\xi(3lVH_0+2tVH_0+ltBH_0+ltBV) - 4tBV\tanh(l\xi/4)} \\ \qquad \times \left(\dfrac{t}{l+t}\right), \qquad \text{for } \tau_0 \neq 0, \end{cases} \tag{20}$$

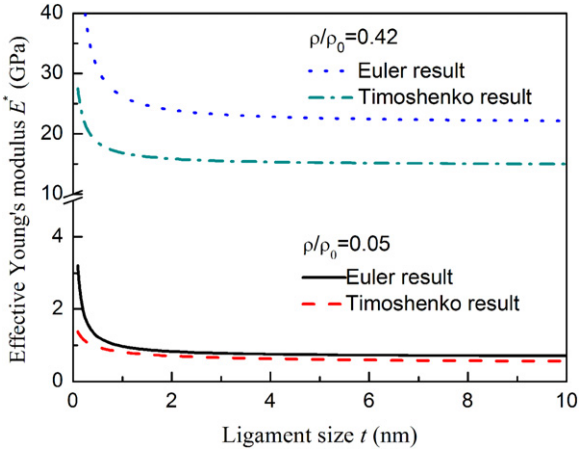

Figure 4. Effective Young's moduli of nanoporous materials predicted by the Euler–Bernoulli model and Timoshenko model.

where $B = E_0t + 4E_s$, $H_0 = 2\tau_0 t$ and $V = \alpha G t^2$. Further, it is noted that the relation between ligament size and relative density for a porous material with a relatively high density ρ/ρ_0 is different from that in low density $(\rho/\rho_0 = (t/l)^2)$, which is given by [10, 12]

$$\frac{\rho}{\rho_0} = \frac{(t/l)^2(1+0.766t/l)}{0.766(1+t/l)^3}. \tag{21}$$

4.2. Example and discussion

To compare the effective elastic moduli predicted by the Euler–Bernoulli and Timoshenko nanobeam models, we choose nanoporous gold as an example. We still use the material constants for the single-crystal Au given in section 3.2. To illustrate the effect of the relative mass density, we give the calculation results in figure 4 under two representative values of $\rho/\rho_0 = 0.05$ and 0.42.

It is found from figure 4 that for a low mass density (e.g. $\rho/\rho_0 = 0.05$), the elastic moduli of nanoporous gold predicted by the two models are very close to each other, whereas for a high density (e.g. $\rho/\rho_0 = 0.42$), the effects of shear deformation on the elastic modulus are significant. It is also clearly seen from figure 3 that the effective elastic modulus predicted by the Timoshenko nanobeam model is always lower than that by the Euler–Bernoulli model. Their difference is especially obvious for nanoporous gold with a high mass density. A similar trend is observed for the influence of surface effects. The above results suggest that the Timoshenko nanobeam model should be applied to predict the elastic properties of nanoporous gold with a relatively higher mass density (e.g. $\rho/\rho_0 > 0.3$) [11, 12], while the simpler Euler–Bernoulli model can be used when the mass density is lower.

5. Elastic buckling of nanoporous materials

When a nanoporous material is subjected to compressive loading, elastic buckling may occur in its ligaments, leading to microstructural collapse. The critical stress for an open-cell porous material at the occurrence of collapse is given by

Gibson and Ashby as [11, 12]

$$\sigma_{\rm el}^0 = \frac{2\pi^2 E_0 t^4}{3l^4} \approx C_4 E_0 \left(\frac{\rho}{\rho_0}\right)^2, \tag{22}$$

where $C_4 = 0.05$ is a proportional constant fitted by experimental data and, sometimes, referred to as the critical buckling strain.

The unit-cell model in figure 1 is used again. Assume the compressive force P is acting on the ligaments in group (i). The elastic collapse under axial compression is mainly triggered by the elastic buckling of the four ligaments in group (ii) [14]. When neglecting the surface effects, the critical buckling load of the ligaments is

$$P_{\rm cr} = \begin{cases} \dfrac{n^2\pi^2 E_0 I}{l^2}, & \text{(Euler model)}, \\ \dfrac{n^2\pi^2 V E_0 I}{Vl^2 + 4\pi^2 E_0 I}, & \text{(Timoshenko model)} \end{cases} \tag{23}$$

where n is a dimensionless parameter depending on the boundary conditions. In the case of a doubly clamped beam, $n = 2$, and I is the second moment of area. Converting the load into stress, the macroscopic average stress $\sigma_{\rm el}$ is obtained as

$$\sigma_{\rm el} = \begin{cases} \dfrac{4\pi^2 E_0 I}{l^2(l+t)^2}, & \text{(Euler model)}, \\ \dfrac{\pi^2 V E_0 I}{(l+t)^2(Vl^2+4\pi^2 E_0 I)}, & \text{(Timoshenko model)}. \end{cases} \tag{24}$$

For nanoporous materials, we here account for the influence of surface effects and denote the critical average stress at the occurrence of microstructural collapse as $\sigma_{\rm el}^*$. Based on our analysis in section 4.1, the critical load $P_{\rm cr}$ at the occurrence of compressive buckling in the e–h ligaments predicted by the Euler–Bernoulli and Timoshenko nanobeam models is [34, 37]

$$P_{\rm cr}^* = \begin{cases} \dfrac{4\pi^2 (EI)^*}{l^2} + H_0, & \text{(Euler model)}, \\ \dfrac{4\pi^2 V (EI)^*}{Vl^2 + 4\pi^2 (EI)^*} + H_0, & \text{(Timoshenko model)}, \end{cases} \tag{25}$$

respectively, where $(EI)^* = E_0 t^4/12 + 2E_{\rm s} t^3/3$, $H_0 = 2\tau_0 t$, $V = \alpha G t^2$ and the boundary conditions are two fixed ends. The macroscopic average stress of a unit cell is $\sigma_{\rm el}^* = 4P_{\rm cr}/(2l+2t)^2$. Thus, the critical average stress on the unit cell of nanoporous materials at the occurrence of microstructural collapse is

$$\sigma_{\rm el}^* = \begin{cases} \dfrac{H_0 l^2 + 4\pi^2 (EI)^*}{(l+t)^2 l^2}, & \text{(Euler model)}, \\ \dfrac{1}{(l+t)^2}\left[\dfrac{4\pi^2 V (EI)^*}{Vl^2 + 4\pi^2 (EI)^*} + H_0\right], & \text{(Timoshenko model)}. \end{cases} \tag{26}$$

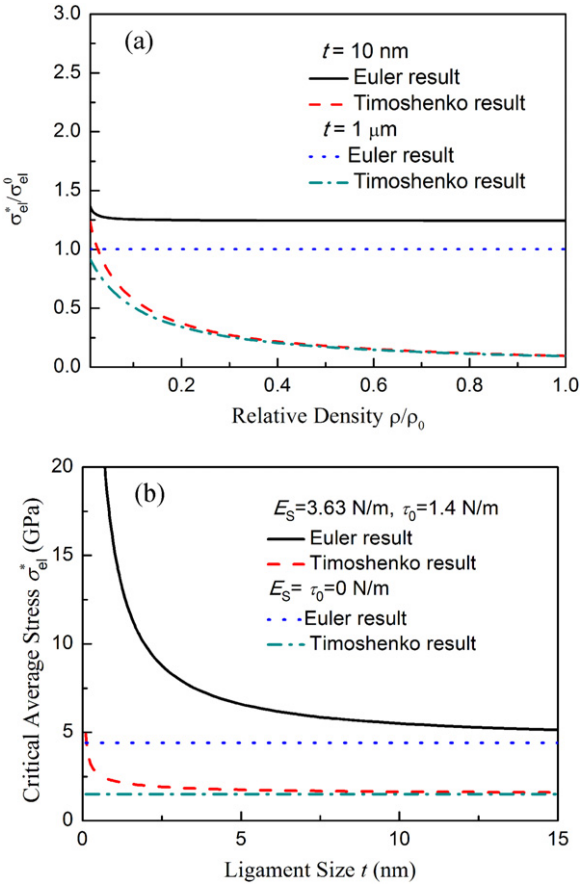

Figure 5. The critical average stresses of ligament buckling predicted by the Euler–Bernoulli model and Timoshenko model with respect to (a) the relative mass density and (b) the ligament size.

To illustrate the difference between the critical average stresses predicted by Euler–Bernoulli and Timoshenko nanobeam models with surface effects, nanoporous gold with a relative density $\rho/\rho_0 = 0.2$ is taken as an example. The curves of the critical average stresses predicted by the two models are plotted in figure 5 as a function of the relative density and the ligament size. In figure 5(a), $\sigma_{\rm el}^0$ denotes the critical average stress of an open-cell foam and is defined by the first expression in equation (24) and the relative density is determined by $\rho/\rho_0 = (t/l)^2$ [11]. Figure 5 shows that the critical average stress exhibits a distinct dependence on the ligament size of nanoporous materials and the surface effects are more significant when the relative density is lower than 0.2. In addition, the influence of shear deformation is prominent for a nanoporous material with a comparatively high relative density.

From figure 5(b), we find that the dependence of the critical average stress on the ligament size of nanoporous gold is similar to that of the elastic modulus depicted in figure 4. The critical average stress shows a distinct increase as the ligament size falls into the scope of several nanometers. Within this scope, the rate of increase of the Timoshenko results with decreased ligament size is much lower than that of the Euler results.

6. Conclusions

By including Gurtin–Murdoch's theory of surface elasticity into the classical Timoshenko beam model, we have presented a size-dependent Timoshenko nanobeam model. Thereby, we have investigated the surface effects on the effective mechanical behavior of nanoporous materials. In particular, we compared the results given by the nanoscale Euler–Bernoulli model and the Timoshenko model. When the average characteristic size of the ligaments in a porous material reduces to nanometers, the effects of surface stresses and surface elasticity become significant and should be taken into account. For nanoporous materials with a low density, the Euler–Bernoulli nanobeam model is appropriate to predict the effective elastic modulus and the critical stress of microstructural buckling, while for those with a high density, the refined Timoshenko model should be used to account for the effect of shear deformation. This study extends the classical Gibson and Ashby's theory for conventional porous materials. In this paper, our attention has been paid mainly to the elastic deformation behavior of nanoporous materials, and further theoretical and experimental effort will be directed towards their plastic properties.

Acknowledgments

The supports from the National Natural Science Foundation of China (grant nos. 10972121, 10972113, 10732050, 10732080, 10772093 and 10802099), the Ministry of Education (SRFDP 20090002110047), the 973 program of MOST (2010CB631005 and 2007CB36803) and the Subject Leaders Plan of Wuhan (201051730545) are acknowledged.

References

[1] Ding Y and Chen M W 2009 *MRS Bull.* **34** 569
[2] Biener J *et al* 2009 *Nat. Mater.* **8** 47
[3] Tappan B C, Steiner S A III and Luther E P 2010 *Angew. Chem. Int. Edn* **49** 4544
[4] Tao Y S, Endo M, Inagaki M and Kaneko K 2011 *J. Mater. Chem.* **21** 313
[5] Narayan R J, Aggarwal R, Wei W, Jin C, Monteiro-Riviere N A, Crombez R and Shen W D 2008 *Biomed. Mater.* **3** 034107
[6] Fujita T, Okada H, Koyama K, Watanabe K, Maekawa S and Chen M W 2008 *Phys. Rev. Lett.* **101** 166601
[7] Xia R, Wang J L, Wang R Y, Li X D, Zhang X, Feng X Q and Ding Y 2010 *Nanotechnology* **21** 085703
[8] Weissmüller J, Newman R C, Jin H J, Hodge A M and Kysar J W 2009 *MRS Bull.* **34** 577
[9] Hodge A M, Biener J, Hayes J R, Bythrow P M, Volkert C A and Hamza A V 2007 *Acta Mater.* **55** 1343
[10] Dou R, Xu B J and Derby B 2010 *Scr. Mater.* **63** 308
[11] Gibson L J and Ashby M F 1997 *Cellular Solids: Structures and Properties* (Cambridge: Cambridge University Press)
[12] Gibson L J and Ashby M F 1982 *Proc. R. Soc.* A *Soc. A—Math. Phys. Eng. Sci.* **382** 1782
[13] Duan H L, Wang J, Karihaloo B L and Huang Z P 2006 *Acta Mater.* **54** 2983
[14] Feng X Q, Xia R, Li X D and Li B 2009 *Appl. Phys. Lett.* **94** 011916
[15] Ouyang G, Yang G W, Sun C Q and Zhu W G 2008 *Small* **4** 1359
[16] Timoshenko S P and Gere J M 1961 *Theory of Elastic Stability* (New York: McGraw-Hill)
[17] Hutchinson J R 2001 *J. Appl. Mech.* **68** 87
[18] Ma H M, Gao X L and Reddy J N 2008 *J. Mech. Phys. Solids* **56** 3379
[19] Zhang J and Liu F 2008 *Appl. Phys. Lett.* **92** 021905
[20] Wang C M, Zhang Y Y and He X Q 2007 *Nanotechnology* **18** 105401
[21] Mindlin R D and Eshel N N 1968 *Int. J. Solids Struct.* **4** 109
[22] Fleck N A and Hutchinson J W 1997 *Adv. Appl. Mech.* **33** 295
[23] Eringen A C 1999 *Microcontinuum Field Theories: Foundations and Solids* (New York: Springer)
[24] Odegard G M, Gates T S, Nicholson L M and Wise K E 2002 *Compos. Sci. Technol.* **62** 1869
[25] Eringen A C and Edelen D G B 1972 *Int. J. Eng. Sci.* **10** 233
[26] Reddy J N and Pang S D 2008 *J. Appl. Phys.* **103** 023511
[27] Adali S 2009 *Nano Lett.* **9** 1737
[28] Gurtin M E, Weissmüller J and Larche F 1998 *Phil. Mag.* A **78** 1093
[29] Miller R E and Shenoy V B 2000 *Nanotechnology* **11** 139
[30] Wang G F and Feng X Q 2007 *Appl. Phys. Lett.* **90** 231904
[31] He J and Lilley C M 2008 *Nano Lett.* **8** 1798
[32] He J and Lilley C M 2008 *Appl. Phys. Lett.* **93** 263108
[33] Zhang T Y, Luo M and Chan W K 2008 *J. Appl. Phys.* **103** 104308
[34] Wang G F and Feng X Q 2009 *Appl. Phys. Lett.* **94** 141913
[35] Ouyang G, Wang C X and Yang G W 2009 *Chem. Rev.* **109** 4221
[36] Shenoy V B 2005 *Phys. Rev.* B **71** 094104
[37] Wang G F and Feng X Q 2009 *J. Phys. D: Appl. Phys.* **42** 155411